Modeling myofilament glycation and reduced cardiovagal baroreflex sensitivity in a multiscale diabetic model of the left ventricle

AnMei Little & Fanny Cheung (BME '22)
BENG 458 Final Project
May 10, 2022

Background and Motivation

Type 2 diabetes mellitus affects approximately 500 million people worldwide. Furthermore, patients with diabetes double their risk of developing heart failure (HF). Researchers have focused on targeting underlying molecular mechanisms that could decouple the effects of diabetes on heart failure. Papadaki et al. (2021) proposed that the amount of methylglyoxal (MG) glycation of actin filament of the sarcomere is a viable biomarker for the eventual development of heart failure in diabetic patients. Essentially, MG glycation of the actin filament decreases the rate constant for the tropomyosin protein from transitioning from the blocked to the open state which inhibits myosin binding and sarcomere contraction. Papadaki et al. (2021) counteracts the inhibitory effect of MG glycation by implementing a thin-filament interacting peptide of myosin binding protein C (cMyBPC) which alters tropomyosin's position on actin allowing a higher probability of myosin binding to the thin filament, effectively rescuing calcium sensitivity of the system. In hopes of understanding the underlying mechanism that connects diabetes to heart failure, we plan to base our multiscale model on this molecular mechanism. At the macroscopic level, it will be interesting to see how heart rate, calcium transience, myofilament contractility, and arterial pressure, for instance, will be affected by the known kinetic rate changes caused by MG glycation.

However, at the macroscopic level, the implementation of a cardiovascular system model that examines the effects of MG glycation will also have to factor in the effects of the baroreflex. Baroreceptors, *in vivo,* reside in the aortic arch and carotid sinuses and signal to the medulla at variable rates that correspond to the changes in arterial pressure. The baroreflex is responsible for modulating a balance between the sympathetic and parasympathetic responses to a change in the system which consists of adjustments in heart rate, contractility, and vascular function and tone. According to Sakamoto et al. (2019), there is clinical evidence that patients with Type 2 diabetes mellitus can use the reduction of baroreceptor sensitivity (BRS) as a risk factor for cardiovascular events such as arteriosclerotic diseases. The reduction of baroreflex sensitivity leads to an increase in blood pressure variability and hypertension which further reduces baroreflex sensitivity. Sakamoto et al. (2019) also states that early evaluation and preservation of the baroreceptor sensitivity through the use of antihypertensive drugs can be used to prevent those with Type 2 diabetes mellitus from experiencing hypertension or blood pressure variability.

In examining the effects of both MG glycation of actin filament proteins, at a molecular level, and reduced baroreceptor sensitivity, at a macroscopic level, on cardiovascular functions as they relate to Type 2 diabetes mellitus, a clearer understanding of the link between diabetes and the onset of cardiovascular disease can be uncovered. Furthermore, as stated by Sharifi et al. (2021), the use of a multiscale model of the cardiovascular system, specifically one that

incorporates molecular-level mechanisms, will be more applicable for clinical purposes where examining the cell-level and body-level effects induced by pharmaceuticals will be important. In terms of Type 2 diabetes mellitus, it will be especially important for modeling a disease type with such a large patient population to incorporate a multiscale approach that will prove useful for pharmaceutical endeavors in the future.

Specific goal of model building

The goal of the model is to determine the effect of myofilament glycation (actin-myosin behavior) and reduced cardiovagal baroreflex sensitivity to heart behavior in diabetics. The effects on pressure-volume curves and cardiac output should be evaluated. Additionally, it is of interest to determine which of the two simulated alterations contributes more to model behavior.

System and Approach

We will be using a multiscale model from Sharifi et al. 2021 (PyMyoVent - on GitHub) that simulates the left ventricle pumping blood through the systemic circulation. It stems from the "MyoSim model of dynamically-coupled myofilaments (Campbell et al., 2018) with the sophisticated model of myocyte electrophysiology developed by ten Tusscher et al. (2004)." It also incorporates baroreflex control of heart mechanics by using "an afferent signal derived from arterial pressure to drive a kinetic model that mimics the net result of neural processing in the medulla and cell-level responses to autonomic drive."

Previous models assume that contractility changes lead to pressure changes, but in vivo, the baroreceptors in the aorta may cause a feedback system (involving the medulla and sympathetic/parasympathetic system) that doesn't actually lead to large pressure changes. Instead, it could down-regulate processes to compensate for the enhanced forces from myosin heads. Sharifi's model takes baroreceptor regulation into account by implementing it into the model. The baroreflex algorithm monitors arterial pressure and regulates the feedback system that alters heart rate, Ca2+ levels, myofilament contractility, and vascular tone.

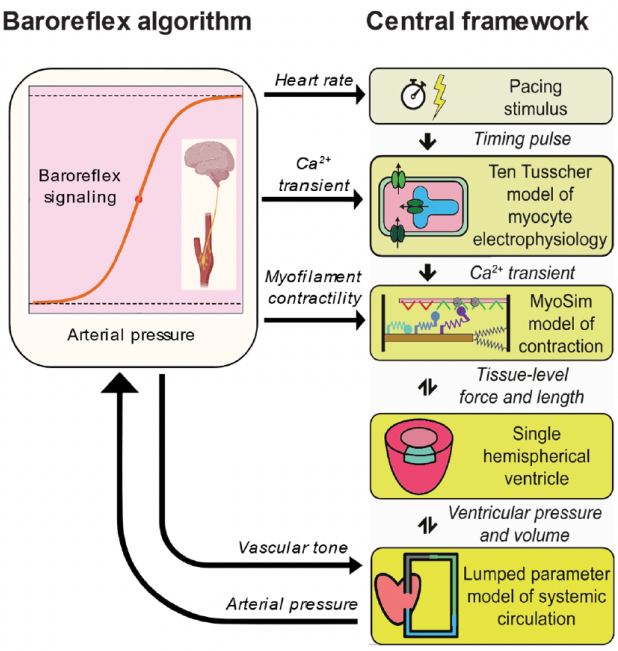

Results of the model simulations show that the baroreflex is able to maintain arterial pressure when blood levels are dropped or when aortic resistance is suddenly increased. If baroreflex is not given control of vascular tone (R and C stay constant), the feedback system is impaired, leading to negative heart mechanics.

The base MyoSim model equations and parameters are pasted below. Further explanation of equations can be found in [Campbell et al. 2020 Supplementary Material].

Thin filament transitions

$$J_{on} = k_{on}\left[Ca^{2+}\right]\left(N_{overlap} - N_{on}\right)\left(1 + k_{coop}\left(\frac{N_{on}}{N_{overlap}}\right)\right)$$

$$J_{off} = k_{off}\left(N_{on} - N_{bound}\right)\left(1 + k_{coop}\left(\frac{N_{overlap} - N_{on}}{N_{overlap}}\right)\right)$$

Thick filament transitions

$$J_1 = k_1(1 + k_{force}F_{total})\,M_{OFF} \qquad J_2 = k_2\,M_{ON}$$

$$J_3(x) = k_3\,e^{\frac{-k_{cb}x^2}{2k_BT}}\,M_{ON}\left(N_{on} - N_{bound}\right) \qquad J_4(x) = \left(k_{4,0} + k_{4,1}\left(x - x_{ps}\right)^4\right)M_{FG}(x)$$

where J1 is the flux of myosin heads transitioning from the M_{OFF} state to the M_{ON} configuration, J2 is the flux of myosin heads into the OFF state, J3 is the flux of myosin heads bound to actin, and J4 is the flux through the myosin detachment step.

The kinetic and force equations used were as follows:

$$\frac{dN_{off}}{dt} = -J_{on} + J_{off}$$

$$\frac{dN_{on}}{dt} = J_{on} - J_{off}$$

$$\frac{dM_{OFF}}{dt} = -J_1 + J_2$$

$$\frac{dM_{ON}}{dt} = \left(J_1 + \sum_{i=1}^{n} J_{4,x_i}\right) - \left(J_2 + \sum_{i=1}^{n} J_{3,x_i}\right)$$

$$\frac{dM_{FG,i}}{dt} = J_{3,x_i} - J_{4,x_i} \quad \text{where} \quad i=1\ldots n$$

$$F_{total} = F_{active} + F_{passive}$$

where

$$F_{active} = N_0 k_{cb} \sum_{i=1}^{n} M_{FG,i}\left(x_i + x_{ps}\right) \qquad F_{passive} = \sigma\left(e^{\frac{x_{hs} - L_{slack}}{L}} - 1\right)$$

$$ATP_{ase} = \frac{N_0\, W_{volume}\, \Delta G`}{L_0\, N_A} \sum_{i=1}^{n} J_{4,x_i}$$

Circulation equations (volume and flow)

$$\frac{dV_{aorta}}{dt} = Q_{ventricle\ to\ aorta} - Q_{aorta\ to\ arteries}$$

$$\frac{dV_{arteries}}{dt} = Q_{aorta\ to\ arteries} - Q_{arteries\ to\ arterioles}$$

$$\frac{dV_{arterioles}}{dt} = Q_{arteries\ to\ arterioles} - Q_{arterioles\ to\ capillaries}$$

$$\frac{dV_{capillaries}}{dt} = Q_{arterioles\ to\ capillaries} - Q_{capillaries\ to\ veins}$$

$$\frac{dV_{veins}}{dt} = Q_{capillaries\ to\ veins} - Q_{veins\ to\ ventricle}$$

$$\frac{dV_{ventricle}}{dt} = Q_{veins\ to\ ventricle} - Q_{ventricle\ to\ aorta}$$

$$Q_{ventricle\ to\ aorta} = \begin{cases} \frac{P_{ventricle} - P_{aorta}}{R_{aorta}} & \text{when} \quad P_{ventricle} \geq P_{aorta} \\ 0 & \text{otherwise} \end{cases}$$

$$Q_{aorta\ to\ arteries} = \frac{P_{aorta} - P_{arteries}}{R_{arteries}}$$

$$Q_{arteries\ to\ arterioles} = \frac{P_{arteries} - P_{arterioles}}{R_{arterioles}}$$

$$Q_{arterioles\ to\ capillaries} = \frac{P_{arterioles} - P_{capillaries}}{R_{capillaries}}$$

$$Q_{capillaries\ to\ veins} = \frac{P_{capillaries} - P_{veins}}{R_{veins}}$$

$$Q_{veins\ to\ ventricle} = \begin{cases} \frac{P_{veins} - P_{ventricle}}{R_{ventricle}} & \text{when} \quad P_{veins} \geq P_{ventricle} \\ 0 & \text{otherwise} \end{cases}$$

The parameter values used are as follows:

Table S1: Base parameter values

Component	Parameter	Value	Units
MyoSim	k_{on}	5×10^8	$M^{-1}\ s^{-1}$
	k_{off}	200	s^{-1}
	k_{coop}	5	Dimensionless
	k_1	2	s^{-1}
	k_2	200	s^{-1}
	k_3	100	$s^{-1}\ nm^{-1}$
	$k_{4,0}$	200	s^{-1}
	$k_{4,1}$	0.1	$s^{-1}\ nm^{-4}$
	k_{cb}	0.001	$pN\ nm^{-1}$
	x_{ps}	5	nm
	$k_{falloff}$	0.0024	nm^{-1}
	σ	500	$N\ m^{-2}$
	L	80	nm
	L_{slack}	900	nm
Ventricle	W_{volume}	0.1	L
	V_{slack}	0.08	L
	$R_{ventricle}$	20	$mm\ Hg\ L^{-1}\ s$
Circulation	V_{total}	5	L
	R_{aorta}	40	$mm\ Hg\ L^{-1}\ s$
	$R_{arteries}$	200	$mm\ Hg\ L^{-1}\ s$
	$R_{arterioles}$	500	$mm\ Hg\ L^{-1}\ s$
	$R_{capillaries}$	300	$mm\ Hg\ L^{-1}\ s$
	R_{veins}	100	$mm\ Hg\ L^{-1}\ s$
	C_{aorta}	0.002	$(mm\ Hg)^{-1}\ L$
	$C_{arteries}$	0.0005	$(mm\ Hg)^{-1}\ L$
	$C_{arterioles}$	0.0005	$(mm\ Hg)^{-1}\ L$
	$C_{capillaries}$	0.0025	$(mm\ Hg)^{-1}\ L$
	C_{veins}	0.35	$(mm\ Hg)^{-1}\ L$

Base values for the electrophysiological model remained as published by ten Tusscher et al. (ten Tusscher et al., 2004).

Changing actin-myosin behaviors (myofilament glycation)

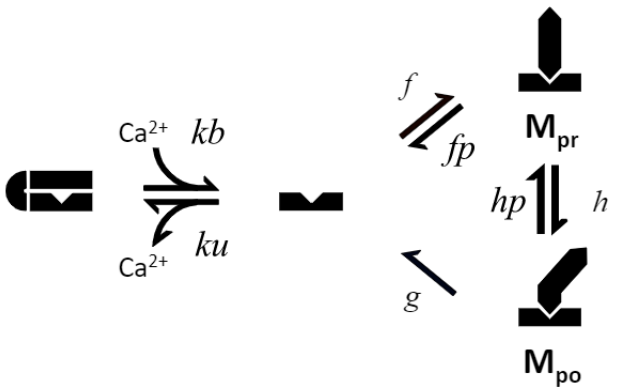

Based on experiments from Papadaki et al. (2019), the myofilament glycation resulted in changes in kinetic rates in the excitation-contraction coupling modeled in the image below. This kinetic scheme of myofilament calcium activation factors in the three tropomyosin states (blocked and calcium-free, blocked and calcium bound, and closed) along with Mpr (the myosin pre-powerstroke) and Mpo (the myosin post-powerstroke) states.

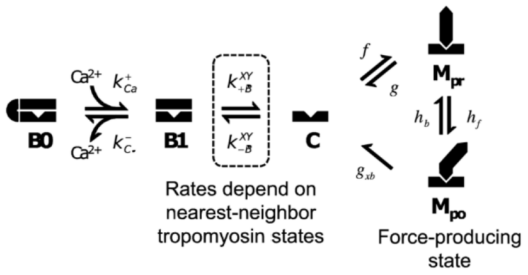

According to Papadaki et al. (2019), using stopped-flow experiments performed on reconstituted regulated thin filaments, myofilament glycation decreased the rate constant (Kb), which describes the transition from the blocked to closed tropomyosin state, by approximately 50%. This is consistent with both the *in vitro* and computational modeling data. By taking this model and decreasing Kb by 50%, we should recapitulate the effect of myofilament glycation.

The following baseline parameters of the myofilament model was taken from the supplemental tables of Sheikh et al. (2012) which is the modified model that was cited in papadaki et al. (2019).

Parameter Name	Values Fitted to Data from Skinned Mouse Myocardium, 15°C	Values Fitted to Data from Intact DM Mouse Papillary Muscle, 25°C	Values Fitted to Data from Intact DM Mouse Papillary Muscle, 37°C	Units
k_{Ca}^{+}	0.09	0.09	0.09	$\mu M\ ms^{-1}$
k_{Ca}^{-}	0.475	0.625	0.625	ms^{-1}
k_{B}^{+}	50	350	750	ms^{-1}
k_{B}^{-}	0.327	0.327	0.327	ms^{-1}
γ_{B}	50	300	300	-
q	0.5	0.5	0.5	-
f	5.1e-03	1.11e-02	0.1	ms^{-1}
g	1.8e-03	7.8e-03	7.0e-02	ms^{-1}
h_f	5.12e-02	0.22	2.0	ms^{-1}
h_b	1.02e-02	3.33e-02	0.4	ms^{-1}
g_{xb}	5.12e-02	0.122	1.1	ms^{-1}
x_0	8	8	8	nm

Parameter Name	Skinned Mouse Myocardium, 15°C $Q_P = 0.39$	Intact WT Mouse Papillary Muscle, 25°C $Q_P = 0.31$	Intact WT Mouse Papillary Muscle, 37°C $Q_P = 0.31$	Units
f	8.4e-03	1.67e-02	0.165	ms^{-1}
h_f	3.59e-02	0.168	1.42	ms^{-1}
h_b	2.97e-02	7.67e-02	1.13	ms^{-1}

<u>Reduced cardiovagal baroreflex sensitivity</u>

Sharifi's model implements baroreflex control through the following equations:

$$\frac{dCa_{SR}(t)}{dt} = k_{SERCA}Ca_{myo}(t) - (k_{leak} + A(t)k_{act})Ca_{SR}(t)$$

$$\frac{dCa_{myo}(t)}{dt} = -\frac{d(Ca_{SR}(t))}{dt}$$

This describes the changes in ca2+ in sarcoplasmic reticulum and in myofilament space, “where the total Ca2+ concentration inside the cell Ca_{total} = Ca_{SR} + Ca_{myo} was kept constant, k_{SERCA} set the rate at which Ca2+ is pumped into the sarcoplasmic reticulum, k_{leak} defines a continual leak of Ca2+ into the myofilament space, and k_{act} controls the release of Ca2+ when the ryanodine receptors are open. A(t) is a pulse wave that is zero except for brief periods of duration t_{open} when A(t) is equal to one. These openings are initiated by the pacing stimuli that occur at time-intervals of t_{RR} and thus determine heart-rate.”

$$B_a(t) = \frac{1}{1+e^{-S(P_{arteries}(t)-P_{set})}}$$

A normalized afferent signal (B_a) was calculated from arterial pressure ($P_{arteries}$) and its setpoint (P_{set}). S defines the slope of the function arounds its midpoint. Sharifi’s simulation involved increasing P_{set} and measuring the resulting heart rate and wall stress.

The model simplifies the process of the medulla modulating sympathetic and parasympathetic efferent signals that increase or decrease arterial pressure. The model uses a “single balance signal B_b, seven distinct control signals ($B_{c,1}$, $B_{c,2}$ …$B_{c,7}$), and seven mapping functions (M_1, M_2 … M_7) [to modulate] ... chronotropism, Ca2+ transients, myofilament function, and vascular tone.” The balance signal represents the difference between the sympathetic and parasympathetic activity, where B_b tends towards 1 when the sympathetic drive dominates and tends towards 0 when the parasympathetic drive dominates. The rate of change in B_b is defined as follows:

$$\frac{dB_b(t)}{dt} = \begin{cases} -k_{drive}(B_a(t) - 0.5)B_b(t) & B_a \geq 0.5 \\ -k_{drive}(B_a(t) - 0.5)(1 - B_b(t)) & B_a < 0.5 \end{cases}$$

The control signals $B_{c,1}$ - $B_{c,7}$ represent the response of seven parameters in the CV model to the balance signal B_b.

$$\frac{dB_{c,i}(t)}{dt} = \begin{cases} k_{control,i}(B_b(t) - 0.5)\left(1 - B_{c,i}(t)\right) & B_b \geq 0.5 \\ k_{control,i}(B_b(t) - 0.5)B_{c,i}(t) & B_b < 0.5 \end{cases}$$

Finally, mapping functions M_1 - M_7 link the normalized control signals $B_{c,I}$ to actual parameter values. The following table displays the mapping relationships.

$$M_i\left(B_{c,i}(t)\right) = \begin{cases} M_{base,i} + \frac{1}{2}(B_{c,i}(t) - 0.5)(M_{symp,i} - M_{base,i}) & B_{c,i} \geq 0.5 \\ M_{base,i} + \frac{1}{2}(B_{c,i}(t) - 0.5)(M_{para,i} - M_{base,i}) & B_{c,i} < 0.5 \end{cases}$$

	Function	Maps to	Increased arterial pressure …
Chrono-tropism	M_1	t_{RR}	Lengthens inter-beat interval and slows heart rate
Calcium-handling	M_2, M_3	k_{SERCA} and k_{act}	Reduces the amplitude and prolongs the duration of Ca^{2+} transients
Sarcomere contractility	M_4, M_5	k_1 and k_{on}	Reduces myosin cycling and sensitizes the thin filaments
Vascular tone	M_6, M_7	$R_{arteriole}$ & C_{veins}	Reduces systemic afterload and increases venous compliance

Table 1: Baroreflex implementation functions

The default parameters used can be found in the supplementary file of the main paper.

List simulations

Through experimental data provided by Papadaki et al. (2019), the main mechanism that myofilament glycation affects actin-myosin interaction is through the decreased rate of tropomyosin transitioning from blocked to closed state (Kb). This will be one of the simulations that we will run to examine changes to calcium sensitivity and force output, at the molecular scale. Another simulation that Papadaki et al. (2019) suggested but was unable to experimentally demonstrate was the role myofilament glycation had on a decrease in the attachment rate of myosin. It was posited that myofilament glycation could enhance the super-relaxed state of myosin resulting in fewer myosin heads available to form crossbridges. This effect would be modeled by a decrease in the rate of attachment (f).

It seems that decreased baroreflex sensitivity can be simulated by altering the $B_{c,i}$ control signals. While the exact mechanism for reduced BRS in diabetic patients is not fully known, it is thought to be independent of impaired glucose tolerance and glycation. Additionally, reductions in BRS start at the earlier stage of diabetes, and thus is probably independent of atherosclerosis, which occurs later on. The Kdrive rate constant sets the speed at which the control signal can respond to a change in arterial pressure. Kdrive can be reduced prior to running the simulation to represent reduced BRS. It has been reported that “reduced BRS leads to an increase in blood pressure variability (BPV), which further leads to reduced BRS.” So maybe even just holding the blood pressure levels higher than homeostasis could induce the reduction in BRS.

*At time = 100s, the resistance of the arterials were reduced by 50% in order to simulate an exercise condition. This condition should emphasize the pathological pre-diabetic conditions.

The outputs measured include heart rate and blood pressure, along with the heart’s pressure-volume curves and cardiac output. By independently varying the myofilament glycation and the baroreflex sensitivity, hopefully we can evaluate the relative contribution of each

alteration to the system's outputs. Additionally, we can check and see if / how they affect one another.

Data sources

The results from clinical studies of patients with Type 2 diabetes mellitus will be necessary data sources to compare the outputs of our multiscale models. At a larger cardiovascular system level, outputs such as heart rate, arterial pressure, and vascular tone need to be compared to clinical baseline measurements of patients with Type 2 diabetes mellitus. Furthermore, clinical data of baseline measurements from patient populations without diabetes but with risks of cardiovascular diseases would be necessary to compare our outputs to. For comparing the results of very specific molecular level adjustments such as the implementation of myofilament glycation, we would compare with experimental values kinetic rates, calcium sensitivity, and force output.

Possible challenges

It may be difficult to be able to distinguish the effects between myofilament glycation and baroreflex sensitivity; however, through a sensitivity analysis, hopefully a general comparison can be made. Other challenges anticipated include determining how much to change the simulation while keeping it within physiological limits. There is limited research on baroreflex sensitivity, and different labs measure it in different ways. Finally, we will likely be adding more limitations to the model (which itself already has limitations). These pre-existing limitations include "the single ventricle architecture, the assumption that the ventricle is hemispherical, and the one-way coupling of the electrophysiological and contractile modules." Being able to develop insightful conclusions from the simulation weighed down by these limitations (and more) may be challenging.

Results

Myofilament Glycation

To confirm that the PyMyoVent system's kinetic model could correlate to the Papadaki et al. model, we decreased the Kon kinetic rate value by 50%, as proposed by Papadaki et al., to create these calcium-force curves.

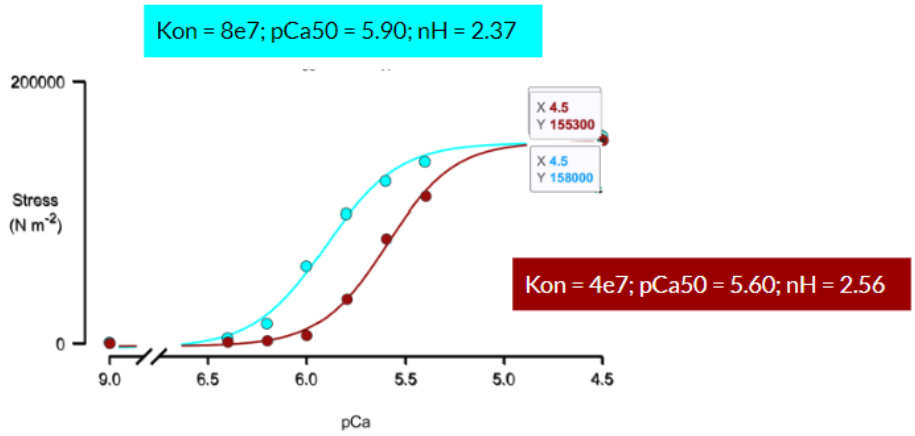

Figure 1. Graph of pCa v. Stress (N/m^2) before and after a 50% decrease in Kon kinetic rate value

We, then, integrated the myofilament glycation into the larger PyMyoVent model. We started with a 50% decrease in the Kon value.

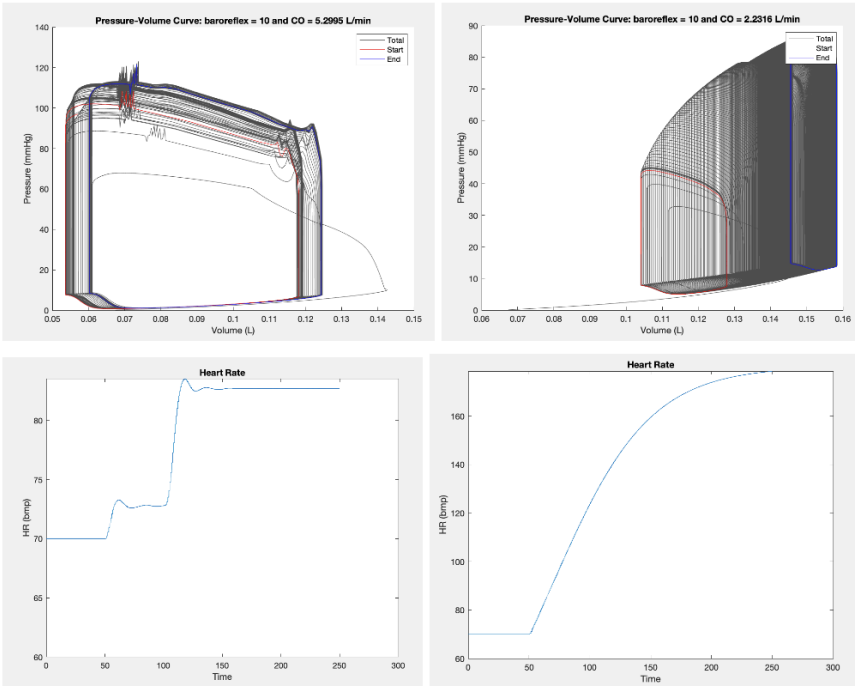

Figure 2. Graphs of PV curves and Heart Rates before and after 50% decrease in Kon kinetic rate value.

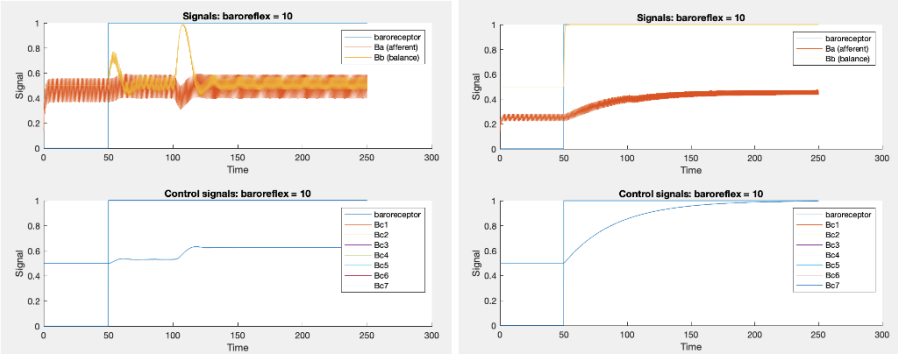

Figure 3. Graphs of baroreflex signals; Normalized afferent signal (B_a), balance signal (B_b), and control signals ($B_{c,1}$, $B_{c,2}$ … $B_{c,7}$) before and after 50% decrease in Kon kinetic rate value.

Then, we modeled a decrease in Kon kinetic rate by 25% to observe the differences.

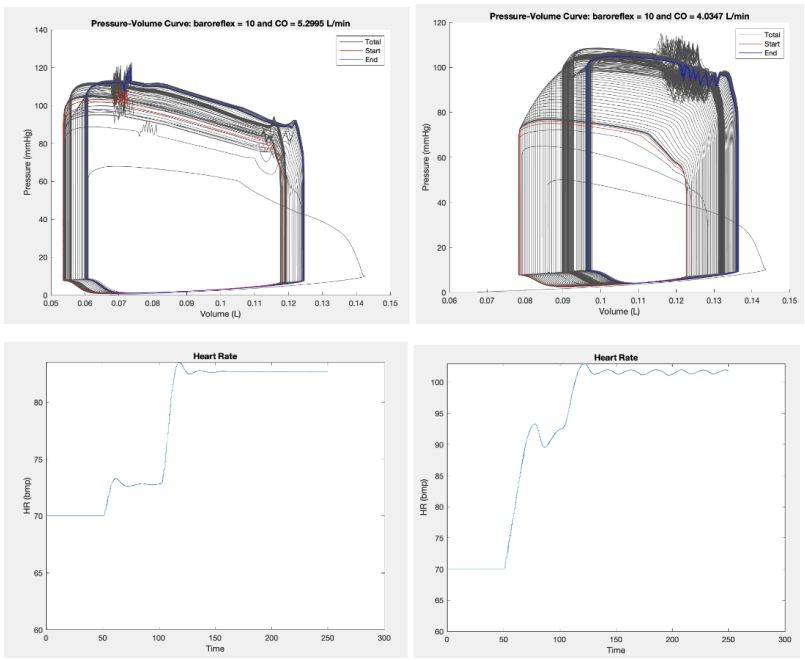

Figure 4. Graphs of PV curves and Heart Rates before and after 25% decrease in Kon kinetic rate value.

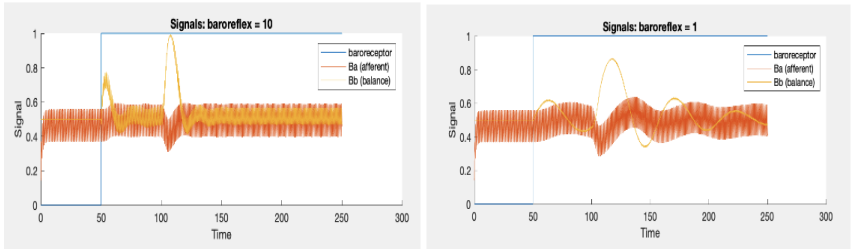

Figure 5. Graphs of baroreflex signals; Normalized afferent signal (B_a), balance signal (B_b), and control signals ($B_{c,1}$, $B_{c,2}$ … $B_{c,7}$) before and after 25% decrease in Kon kinetic rate value.

Baroreceptor Sensitivity

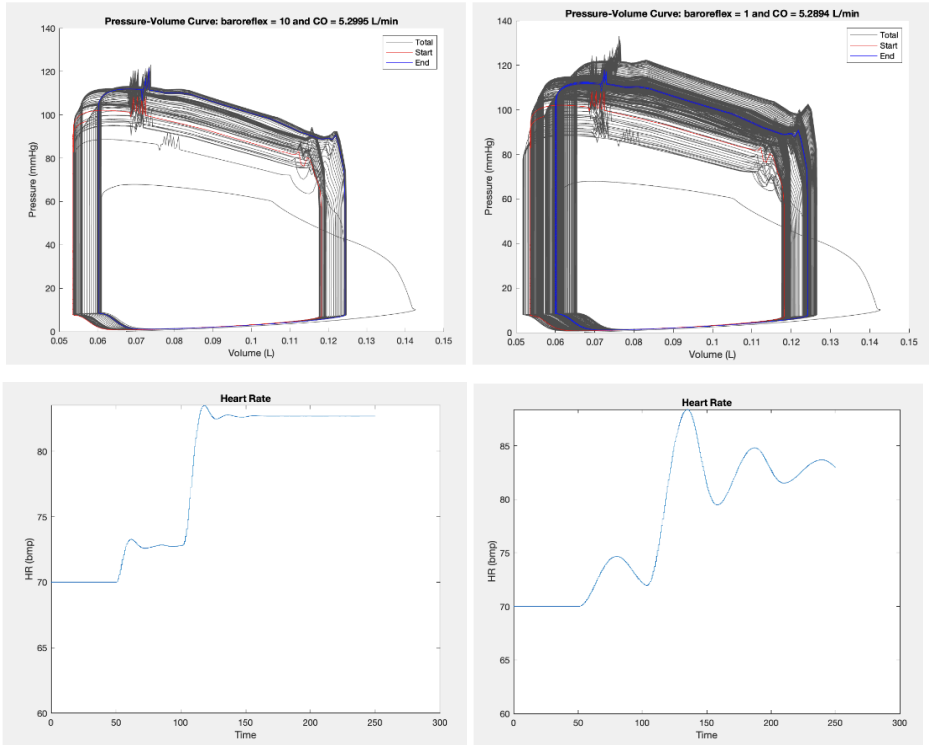

Figure 6. Graphs of PV curves and Heart Rates before and after decreasing baroreceptor sensitivity by 90%.

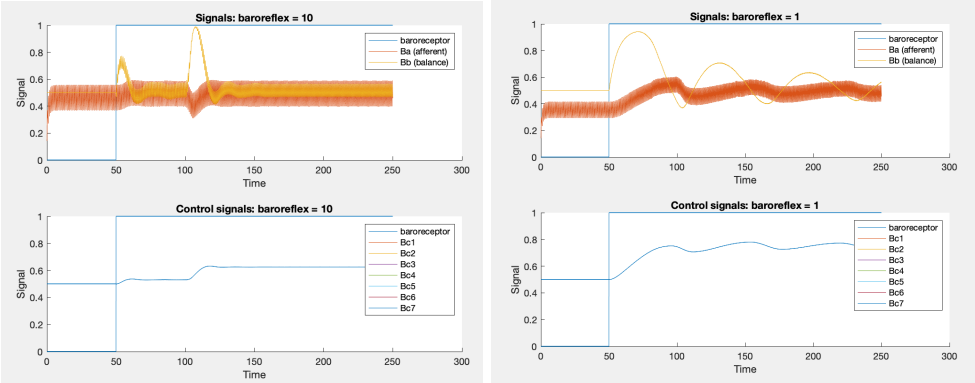

Figure 7. Graphs of baroreflex signals; Normalized afferent signal (B_a), balance signal (B_b), and control signals ($B_{c,1}$, $B_{c,2}$ … $B_{c,7}$) before and after 90% decrease in baroreceptor sensitivity.

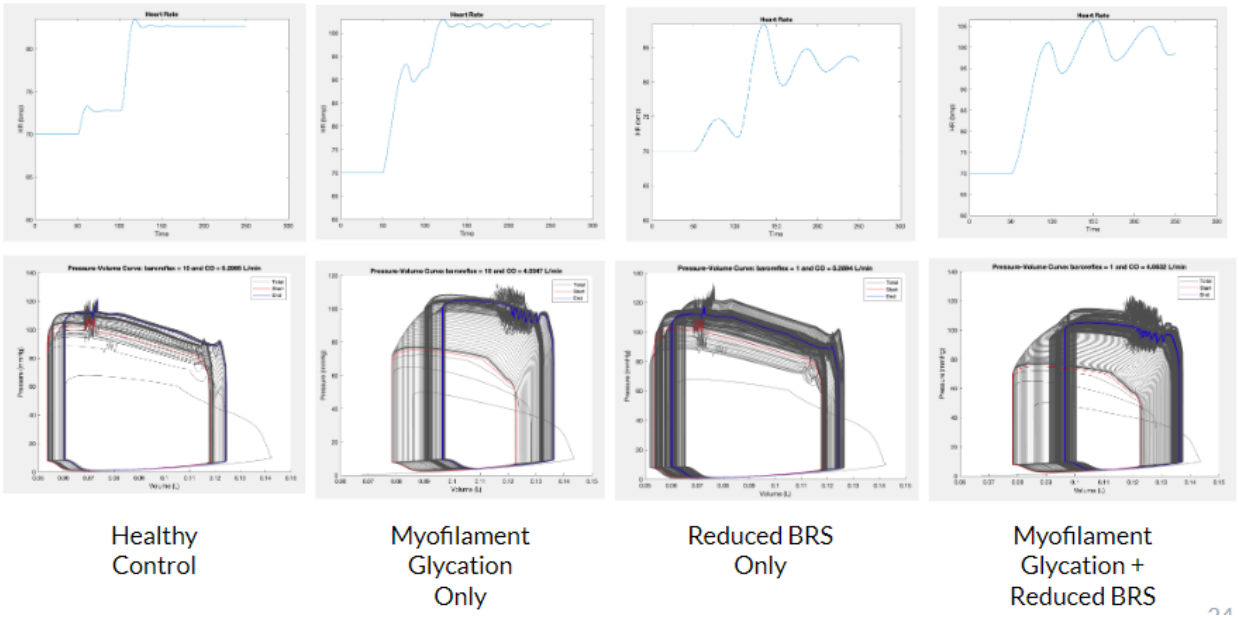

Figure 8. Graphs of PV curves and Heart Rates of a) Healthy Control b) Myofilament Glycation via 25% decrease in Kon only c) 90% Reduction in BRS Only d) MG + Reduced BRS together

Discussion/Conclusion

Using the MATMyoSim model, we first observed what changes would arise from decreasing the Kon kinetic rate. We decreased the Kon kinetic rate by 50% starting with the default value of 8e7 M-1 s-1, and decreasing to a value of 4e7 M-1 s-1. We see in figure 1, the graph of pCa vs. Stress (N*m-2) results in the expected sigmoidal relationship. The 50% decrease in Kon resulted in a decrease in pCa50, also known as the calcium concentration required for 50% of maximum force production, meaning there is decrease in calcium sensitivity.

We then integrated the MATMyoSim model values into the larger PyMyoVent system and decreased the Kon value by 50% to see what effects it would have on cardiac output (CO) and the control signals such as heart rate, vascular tone, and myofilament contractility. We can see that CO decreases from 5.3 L/min to approximately 2.3 L/min according to figure 2. Additionally we see a steadily increasing heart rate in the glycated results. In figure 3, we also see the balance signal (Bb) in the myofilament glycation results approaching 1 which is a measurement of sympathetic response. It makes sense that as myofilament glycation increases, less force production will occur due to the inhibition of tropomyosin movement and thus the heart cannot pump as much blood per heartbeat leading to decreased CO. Similarly, as CO per heartbeat decreases, the heart rate has to continue to increase to pump out more blood in time.

We see very similar results when we decrease the Kon rate by 25% which we see in figures 4 and 5. Understandably, we see a less severe decrease in CO (5.3 L/min to 4.0 L/min) and in figure 5 we no longer see a purely sympathetic response but rather an oscillating balance of parasympathetic and sympathetic responses.

In the case of reduced baroreceptor sensitivity alone, we decreased the baroreceptor sensitivity (BRS) by 90% which resulted in a slight decrease in CO (5.2995 L/min to 5.2894 L/min), according to figure 6.We can also see in figure 6, the heart rate, following exercise conditions being implemented at t = 100 s, in the reduced BRS case is fluctuating to reach steady state again. We can also see in figure 7 that reduced BRS results in an attempt to balance parasympathetic and sympathetic responses as evident by the Bb signal. We can see that the reduced BRS case reaches close to 0.7 in Bb signal similar to the 0.6 value in Bb signal seen in the normal baroreceptor sensitivity case.

When we observe the effect of myofilament glycation (Kon decreased 25%) and reduced BRS (90%) together, we see in figure 8 that myofilament glycation drives changes in CO, while BRS drives large fluctuations in heart rate. Myofilament glycation inhibits myosin heads from binding to actin thus decreasing force output per cardiac cycle. This decrease in force would decrease cardiac output per heartbeat thus, to maintain the same cardiac output in time, the heart rate would have to increase (which is controlled by the baroreceptor starting at t=50s). Furthermore, in an exercise condition (t=100s), the baroreceptor would further increase heart rate.

Limitations

A major limitation of examining the effects of BRS and myofilament glycation together and even separately is that the percentage reduced in each case has no reference point to each other. Meaning, there is a variable scale of impact when moving from the kinetic model to the larger scale model. Without having set values that match experimental data and correctly translate to this multiscale model, the 50% decrease in Kon could translate to a much larger decrease in the larger model. Perhaps the reason we see such a drastic change in CO and other control signals is due to an overrepresentation of myofilament glycation.

Future Directions

To continue examining the effects of myofilament glycation and reduced BRS to heart behavior in this multiscale model of diabetic characteristics, we would want to examine changes in the thick filament kinetic rate for the recovery of calcium sensitivity. Specifically, Papadaki et al. showed data that the use of an n-terminal peptide of myosin-binding protein C could recover calcium sensitivity. We would also like to look at other mechanisms that lead to diabetes or heart failure which could mean examining cardiomyopathies or artheroscleortic conditions.

Sources

A multiscale model of the cardiovascular system that incorporates baroreflex control of chronotropism, cell-level contractility, and vascular tone

Multiscale Modeling of Cardiovascular Function Predicts That the End-Systolic Pressure Volume Relationship Can Be Targeted via Multiple Therapeutic Strategies

“Myofilament glycation in diabetes reduces contractility by inhibiting tropomyosin movement, is rescued by cMyBPC domains”

Arterial stiffness, cardiovagal baroreflex sensitivity and postural blood pressure changes in older adults: the Rotterdam Study

Spontaneous baroreflex sensitivity and its association with age, sex, obesity indices and hypertension: a population study

Clinical Implications of Baroreflex Sensitivity in Type 2 Diabetes

Mouse and computational models link Mlc2v dephosphorylation to altered myosin kinetics in early cardiac disease

Effect of reduced total blood volume on left ventricular volumes and kinetics in type 2 diabetes